RUB

TeVPA 2023

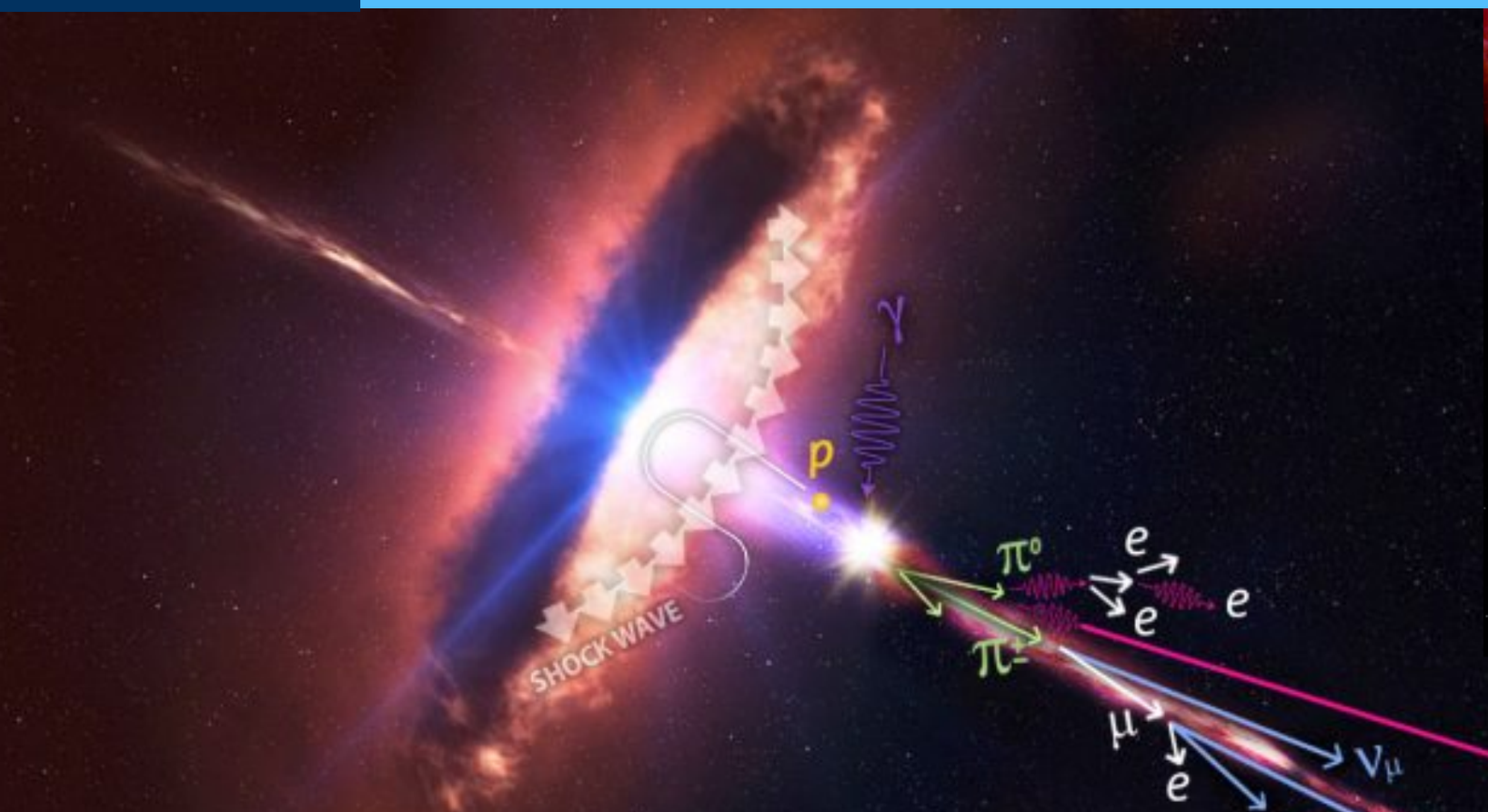

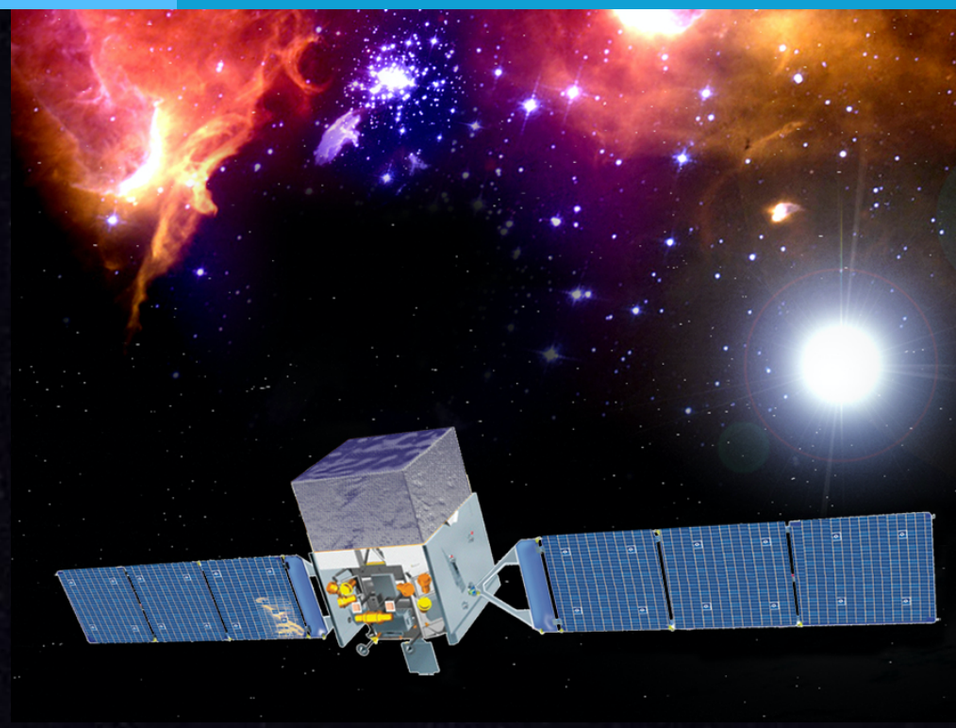

Searching for temporary gamma-ray dark blazars associated with IceCube neutrinos

A&A in print

E. Kun, I. Bartos, J. Becker Tjus, P. L. Biermann,
A. Franckowiak, F. Halzen, Gy. Mező

12/09/2023

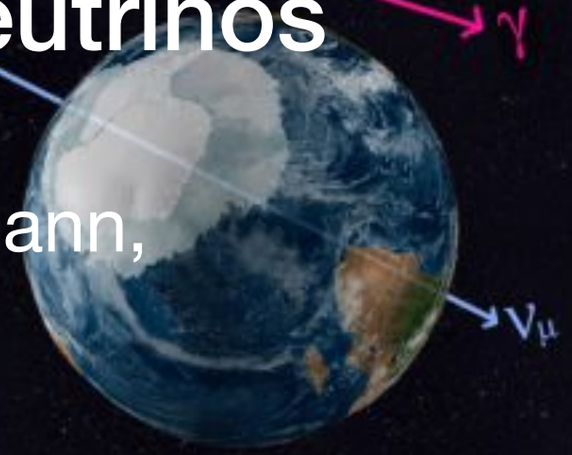

Motivation: Tension between the Fermi diffuse gamma-ray sky and the IceCube neutrino sky

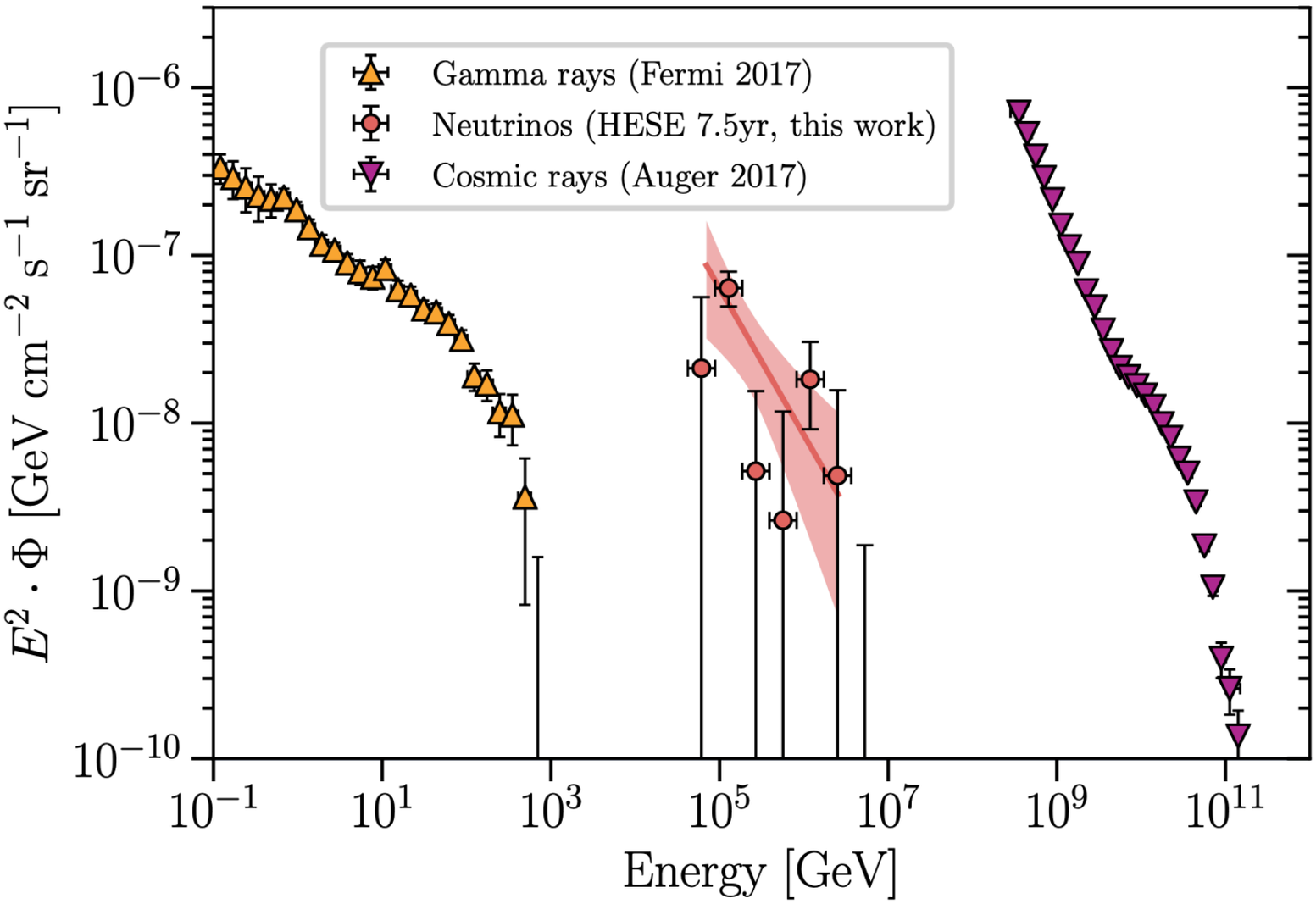

More flux in neutrinos at lower energies that could be expected from gamma-rays, *if* they have the same sources.

The IceCube high-energy starting event sample: Description and flux characterization with 7.5 years of data
IceCube Collaboration, Phys. Rev. D 104, 022002 (2021)

Cosmic Neutrinos from Temporarily Gamma-suppressed Blazars

Kun, Bartos, Becker-Tjus, Biermann, Halzen, Mező, 2021, ApJ, 911,L18

A very interesting FSRQ: PKS 1502+106

- Redshift of **TXS 0506+056** is about **0.336** (**D_L is 1786.8 Mpc** or 5.828 Gly)
  N_{Pred}: 7619.8; Flux(1-100GeV): 8.02e-09 ph/cm^2/s; Peak flux: 1.94e-07 ph/cm2/s

- Redshift of **PKS 1502+106** is about **1.838** (**D_L is 14256.4 Mpc** or 46.498 Gly)
  N_{Pred}: 25352.5; Flux(1-100GeV): 2.02e-08 ph/cm^2/s; Peak flux: 9.72e-07 ph/cm^2/s

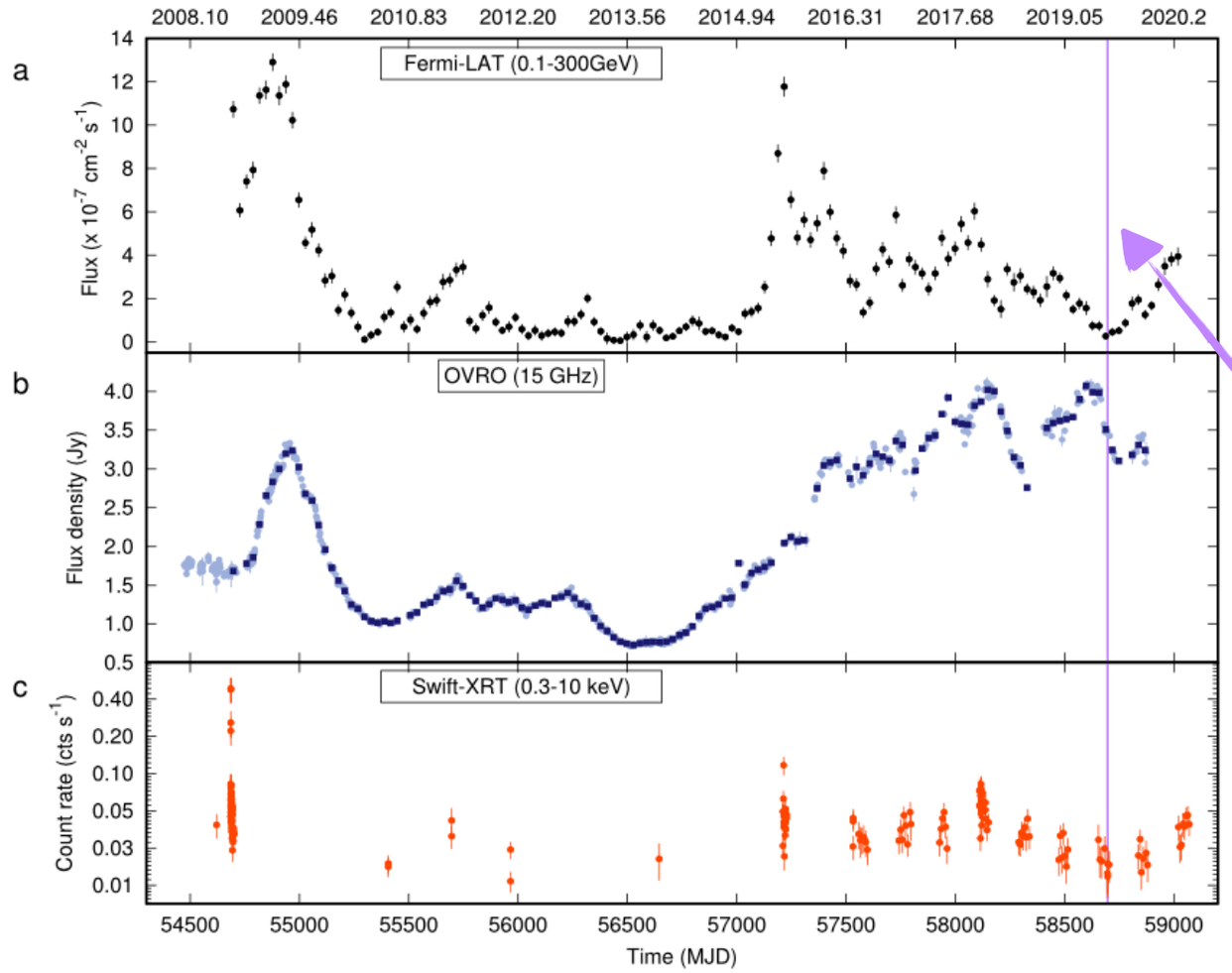

PKS 1502+106 is an exceptionally luminous FSRQ

The associated IceCube neutrino IC-190730A came during a prolonged gamma-ray minimum and peak radio flux density of PKS 1502+106

The proposed scenario

$p\gamma$ in jets, pp is probably subdominant because of the lower particle densities

Transparent mode*

Suppressed mode (gamma-rays cascade down to X-rays)

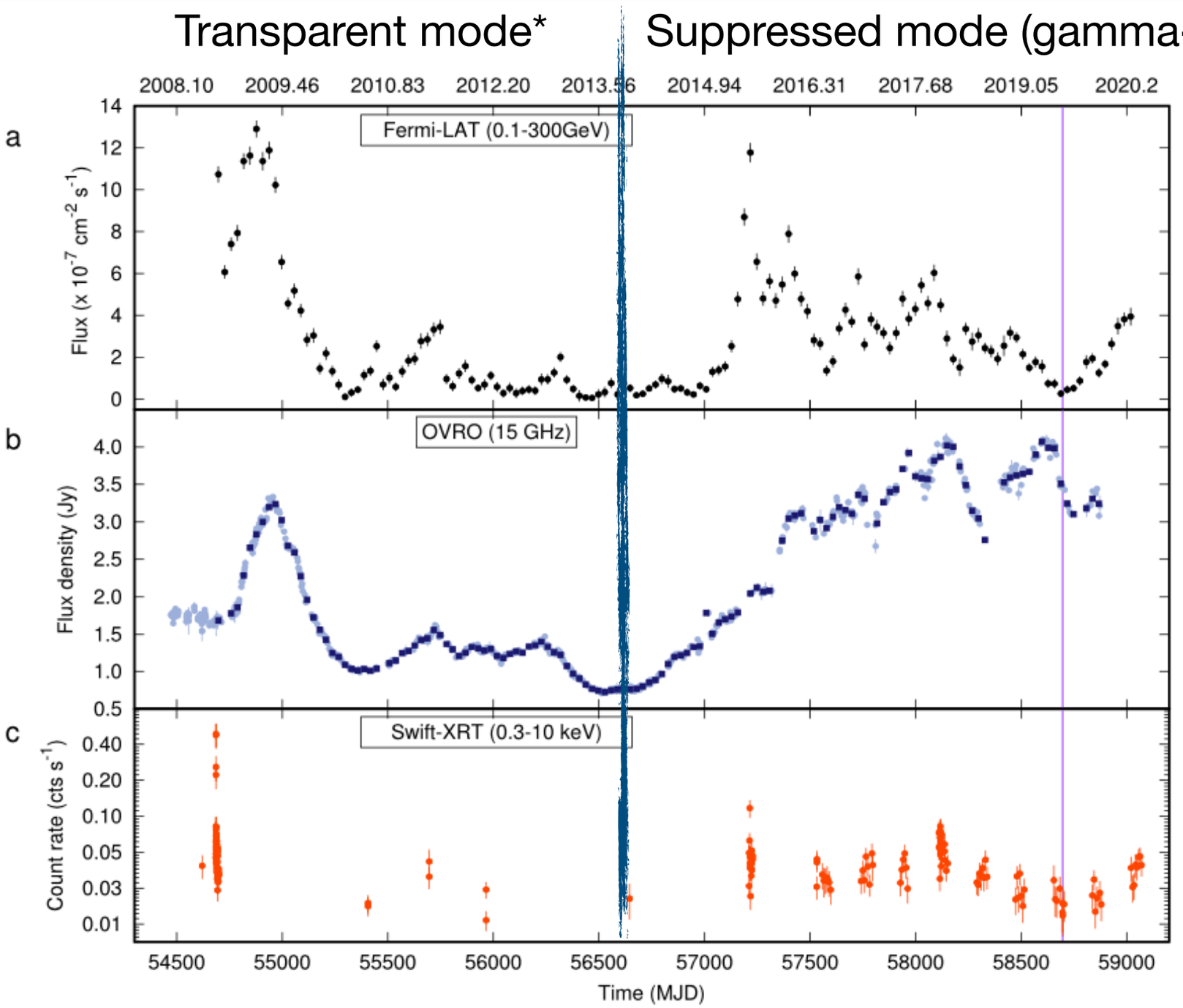

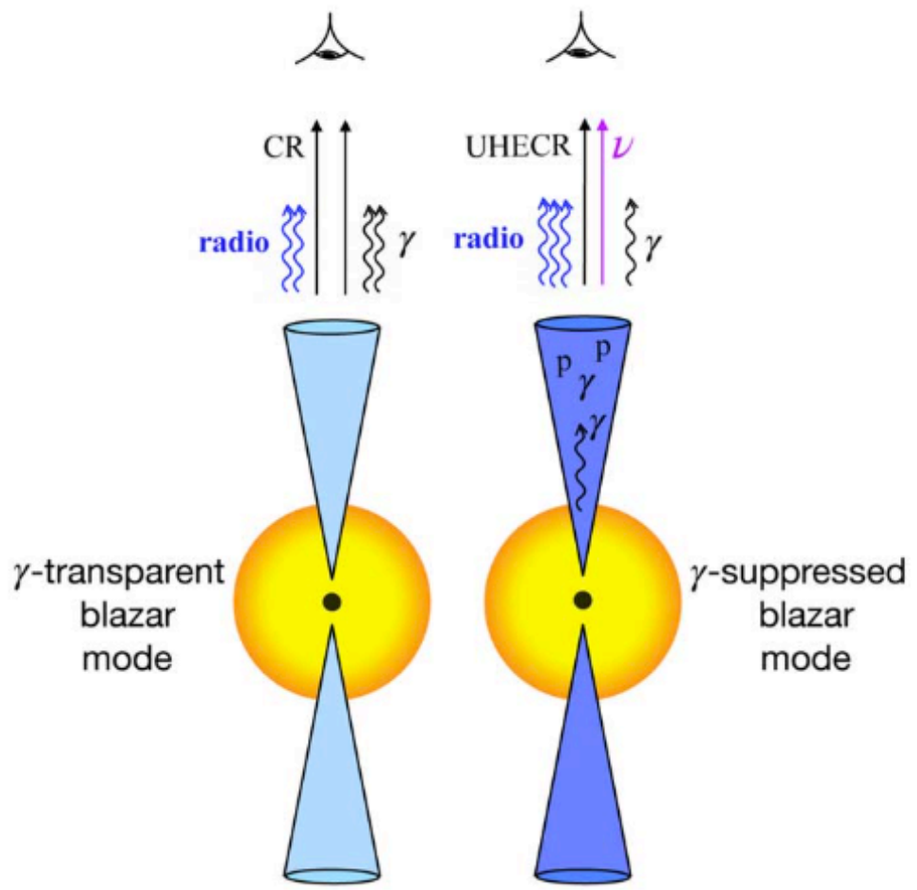

$\tau_{p\gamma} \sim 0.4$ → $\tau_{\gamma\gamma} \sim \mathcal{O}(100)$

*DCF: the radio flux density curve lags behind the gamma-rays with $\Delta\tau = 59 \pm 32$ days

Three examples of recording an IceCube neutrino event during a local or global gamma-ray minimum

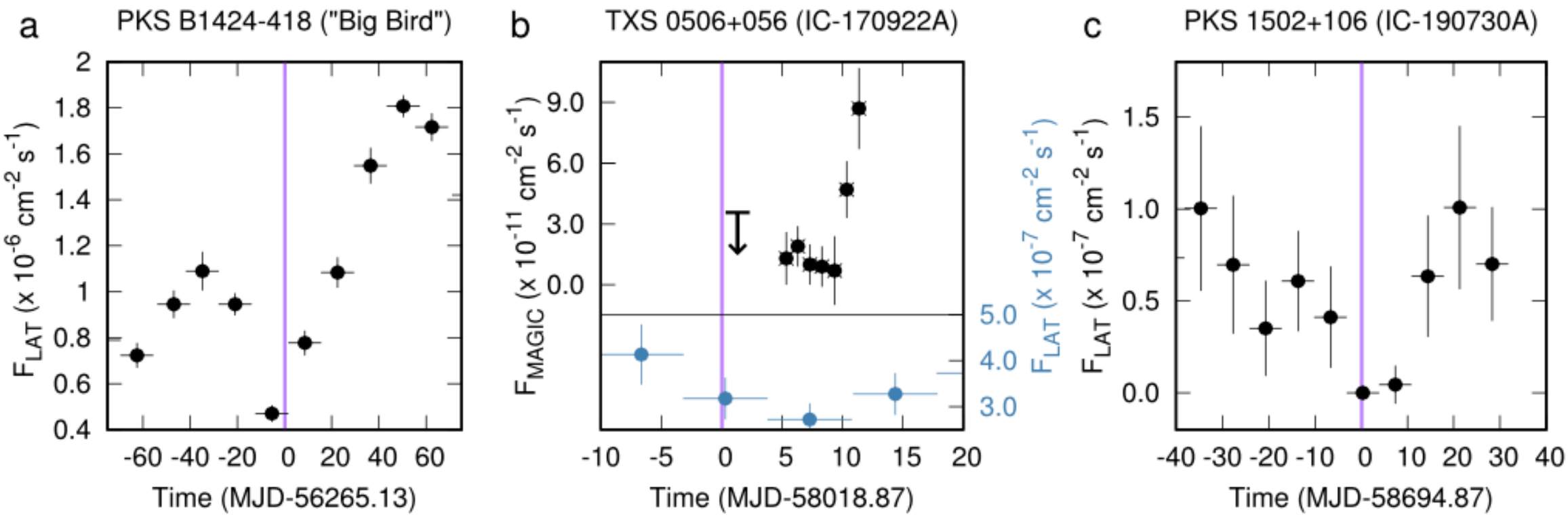

… but we need more

Multiwavelength Search for the Origin of IceCube's Neutrinos

Kun, Bartos, Becker Tjus, Biermann, Franckowiak, Halzen, 2022, ApJ, 934, 180

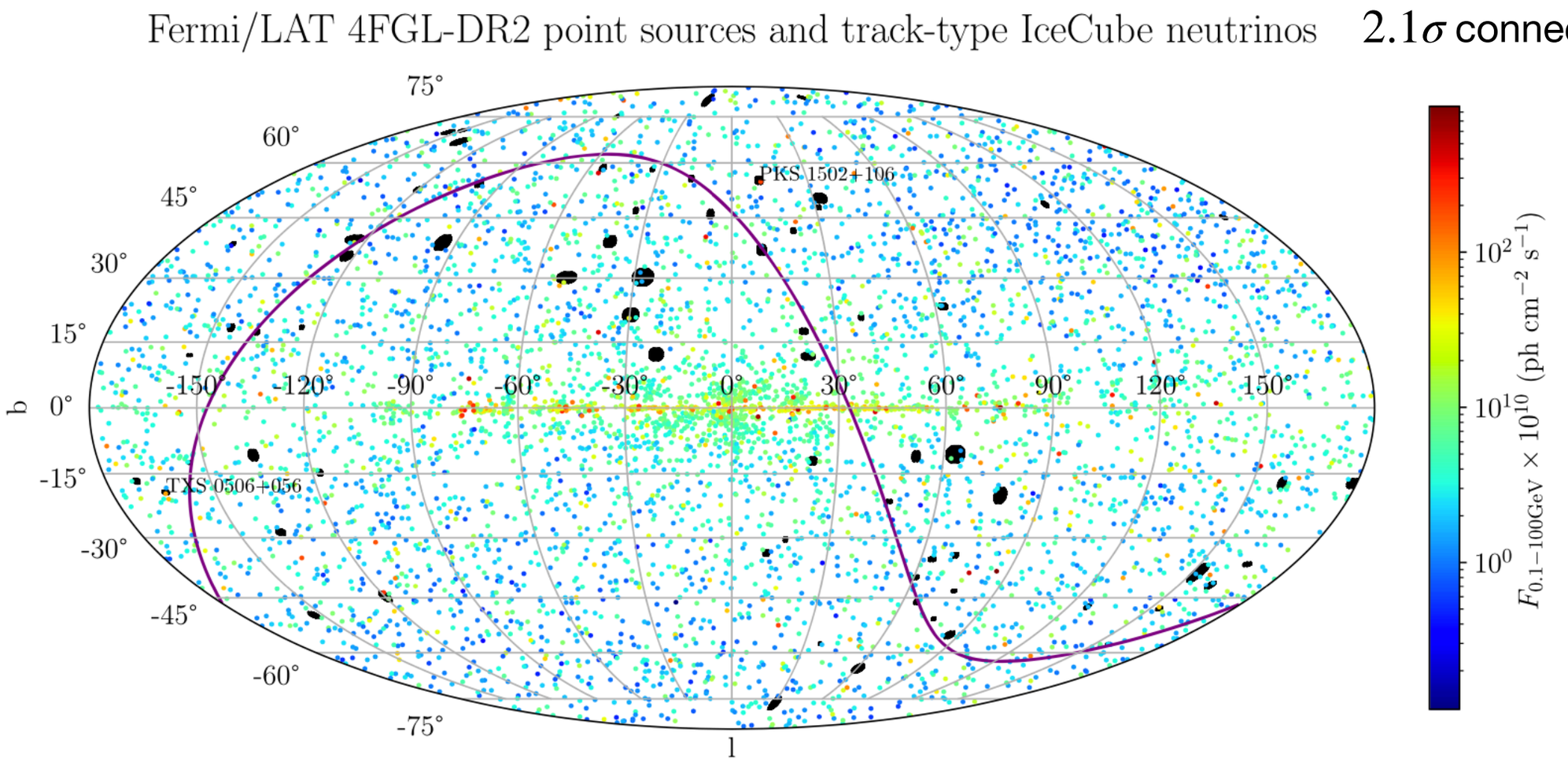

Figure 1. Galactic sky position (l, b) and 0.1 GeV–100 GeV flux ($F_{0.1-100\ \mathrm{GeV}}$) of the Fermi-LAT 4FGL-DR2 point sources (colored dots), overlaid on the list of the 70 track-type neutrino detections by the IceCube Neutrino Detector (black filled ellipses) compiled by Giommi et al. (2020). The map is shown in Mollweide projection. The equator is plotted as a purple continuous line. TXS 0506+056 and PKS 1502+106 are marked on the map. The seven brightest sources (with $F_{0.1-100\ \mathrm{GeV}} > 10^{-7}$ photons cm^{-2} s^{-1}) are not shown in order to enhance the visibility of the flux-diversity of the sources.

● Track neutrinos from the list compiled by Giommi et al. 2020
(70 events from IC-090813A to IC-190730A)

Multiwavelength Search for the Origin of IceCube's Neutrinos

Kun, Bartos, Becker Tjus, Biermann, Franckowiak, Halzen, 2022, ApJ, 934, 180

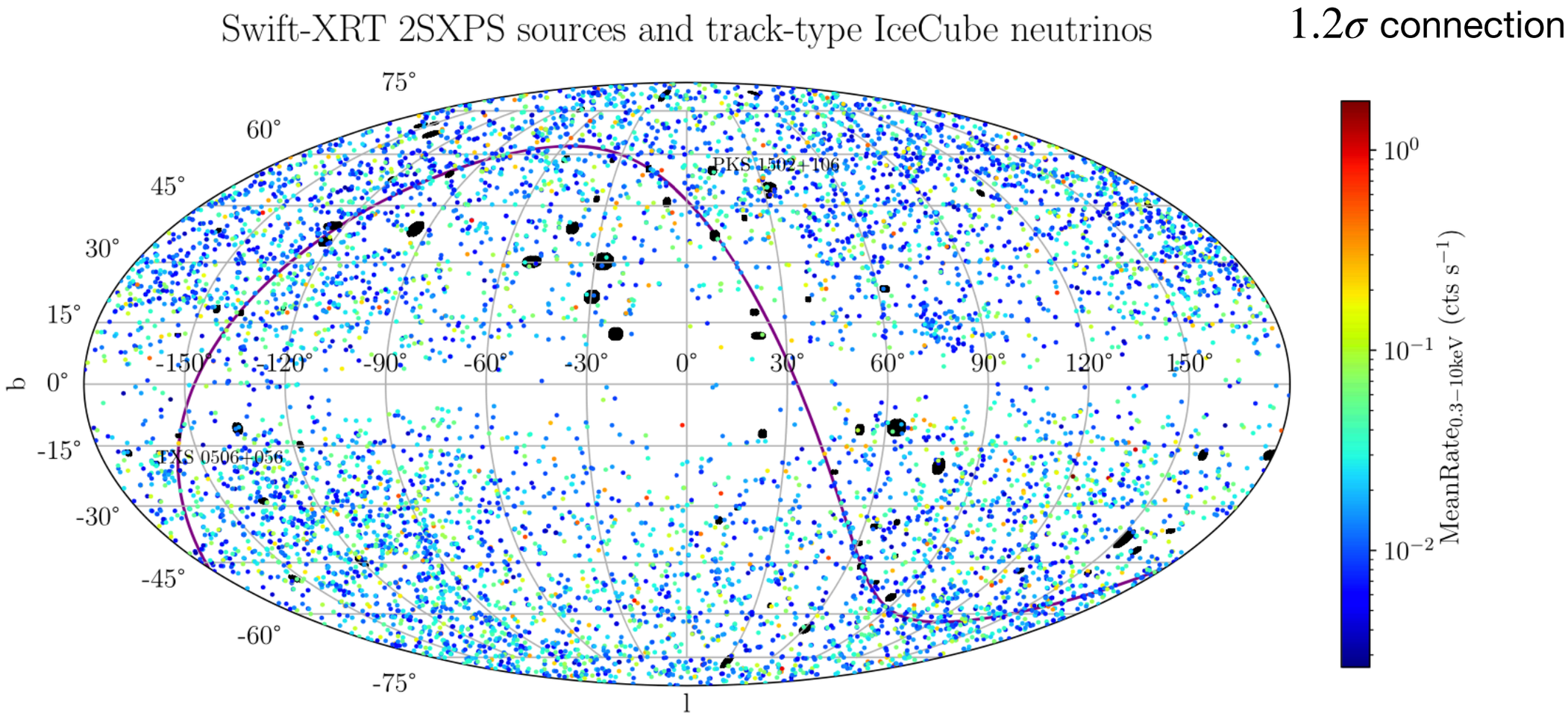

1.2σ connection

Figure 2. Galactic sky position (l, b) and mean rate of the Swift-XRT 2SXPS point sources (S/N $\geqq$ 10, chance of being an AGN is >0.99, colored dots) overlaid on the list of the 70 track-type neutrino detections by the IceCube Neutrino Detector (black filled ellipses) compiled by Giommi et al. (2020). The map is shown in Mollweide projection. The equator is plotted as a purple continuous line. TXS 0506+056 and PKS 1502+106 are marked on the map.

● Track neutrinos from the list compiled by Giommi et al. 2020
(70 events from IC-090813A to IC-190730A)

Multiwavelength Search for the Origin of IceCube's Neutrinos

Kun, Bartos, Becker Tjus, Biermann, Franckowiak, Halzen, 2022, ApJ, 934, 180

2.0σ connection (4.8 GHz)
2.1σ connection (8.4 GHz)

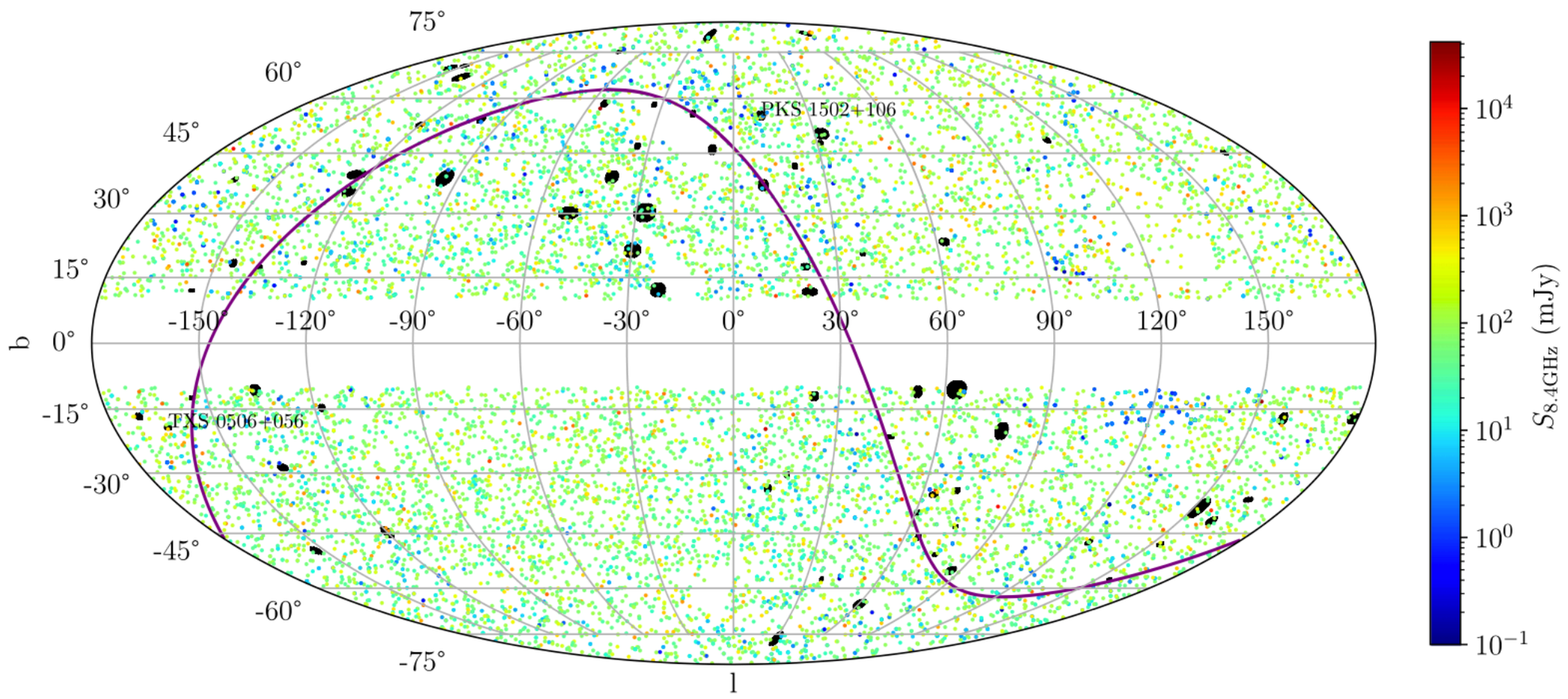

Figure 3. Galactic sky position (l, b) and 8.4 GHz flux density of the CRATES radio sources (colored dots) and list of the 70 track-type neutrino detection by the IceCube Neutrino Detector (black filled ellipses) compiled by Giommi et al. (2020). The maps are shown in Mollweide projection. The equator is plotted as a purple continuous line. TXS 0506+056 and PKS 1502+106 are marked on the map.

● Track neutrinos from the list compiled by Giommi et al. 2020
(70 events from IC-090813A to IC-190730A)

The number of…

Fermi-LAT matches

Swift-XRT matches

CRATES (4.8 GHz) matches

CRATES (8.4GHz) matches

Summary of the Multiwavelength Flux in the Catalogs and for the Multiwavelength ν-samples

	N	$\bar{F}$	σ_F	med(F)	min(F)	max(F)
Fermi-LAT 4FGL: $F_{0.1-100\mathrm{GeV}}$ (photons cm^{-2} s^{-1})	–	(10^{-9})	(10^{-9})	(10^{-10})	(10^{-11})	(10^{-8})
T	5787	1.5	20.8	3.2	1.1	135.2
S	29	2.4	5.6	3.3	3.9	2.4
Swift-XRT 2SXPS: R_m (counts s^{-1}), S/N $\geqq$ 10	N	$\bar{R}_m$	σ_R	med(R_m)	min(R_m)	max(R_m)
T	9097	0.039	0.077	0.015	0.002	1.755
S	61	0.049	0.068	0.027	0.003	0.3603
CRATES: $S_{4.8}$ (mJy)	N	$\bar{S}_{4.8}$	$\sigma_{S4.8}$	med($S_{4.8}$)	min($S_{4.8}$)	max($S_{4.8}$)
T	11,131	251	905	120	65	46, 894
S	87	544	573	232	66	2, 530
CRATES: $S_{8.4}$ (mJy)	N	$\bar{S}_{8.4}$	$\sigma_{S8.4}$	med($S_{8.4}$)	min($S_{8.4}$)	max($S_{8.4}$)
T	14,467	149	596	65	0.1	41, 725
S	96	423	497	171	13.4	1813.4

…with the 70 track neutrinos

Results

1. We found similar levels of correlation between the 70 IceCube neutrinos and gamma-ray, X-ray, and radio source catalogs. Each of these catalogs correlated with neutrino sources at 1.2σ–2.1σ.

2. The subsample of CRATES radio sources complete in radio luminosity can explain between 4% and 53% of the neutrinos at 4.8 GHz and between 3% and 42% of the neutrinos at 8.4GHz (90%C.L. and 50% signalness), when the probability of detecting a neutrino is assumed to be proportional to the (k-corrected) radio flux. This result is consistent with the contribution of AGNs to IceCube's neutrinos based on individually identified sources.

Then we moved to the Fermi-LAT data of neutrino source candidates in the next paper

Searching for temporary gamma-ray dark blazars associated with IceCube neutrinos

(Kun, Bartos, Becker-Tjus, Biermann, Franckowiak, Halzen, Mező, 2023, A&A, in print)

Matched positions of point sources in the Fermi 4FGL-DR2 catalog with track-type neutrinos from Giommi et al. (2020)

Table 1. Source properties of the 29 neutrino source candidates from the 10 years *Fermi*-LAT point–source catalog (4FGL-DR2), published in Kun et al. (2022).

4FGL ID	RA (°)	Dec (°)	N_{pred}	F_{1000} (ph cm^{-2} s^{-1})	F_{peak} (ph cm^{-2} s^{-1})	Class	Association
(1)	(2)	(3)	(4)	(5)	(6)	(7)	(8)
4FGL J2030.5+2235	307.64	22.59	117.0	1.36e-10	–	–	–
4FGL J2030.9+1935	307.74	19.60	526.8	8.24e-10	–	BLL	RX J2030.8+1935
4FGL J1808.2+3500	272.07	35.01	730.8	3.72e-10	1.75e-08	BLL	MG2 J180813+3501
4FGL J1808.8+3522	272.22	35.38	305.6	1.91e-10	–	BLL	2MASX J18084968+3520426
4FGL J1744.2-0353	266.05	−3.89	740.6	3.90e-10	–	FSRQ	PKS 1741-03
4FGL J0230.3+1713	37.60	17.22	537.5	2.52e-10	–	–	–
4FGL J0224.9+1843	36.23	18.72	983.7	1.70e-10	4.52e-08	FSRQ	TXS 0222+185
4FGL J1117.0+2013	169.27	20.23	1442.3	**1.25e-09**	2.09e-08	BLL	RBS 0958
4FGL J2227.9+0036	336.98	0.62	679.9	8.70e-10	–	BLL	PMN J2227+0037
4FGL J1233.0+1333	188.26	13.56	828.0	3.34e-10	–	–	–
4FGL J1040.5+0617	160.15	6.28	2927.1	**1.49e-09**	6.26e-08	BLL	GB6 J1040+0617
4FGL J0854.0+2753	133.52	27.88	28.4	3.93e-11	–	BLL	SDSS J085410.16+275421.7
4FGL J1557.9-0001	239.49	−0.02	412.3	1.86e-10	–	FSRQ	PKS 1555+001
4FGL J1258.7-0452	194.68	−4.87	124.1	1.73e-10	–	BLL	RBS 1194
4FGL J1311.8+2057	197.97	20.96	617.2	5.30e-11	–	BCU	MG2 J131144+2052
4FGL J0103.5+1526	15.88	15.43	294.7	1.74e-10	–	BLL	TXS 0100+151
4FGL J1316.1-3338	199.03	−33.64	3866.4	**2.39e-09**	1.22e-07	FSRQ	PKS 1313-333
4FGL J0244.7+1316	41.19	13.28	574.5	2.01e-10	1.78e-08	Blazar	GB6 J0244+1320
4FGL J1447.0-2657	221.77	−26.96	195.1	1.64e-10	–	BCU	NVSS J144657-265713
4FGL J1439.5-2525	219.88	−25.42	153.9	1.55e-10	–	BCU	NVSS J143934-252458
4FGL J0509.4+0542	77.36	5.70	7619.8	**8.02e-09**	1.94e-07	BLL	TXS 0506+056
4FGL J1457.4-3539	224.37	−35.65	5233.2	**3.49e-09**	2.56e-07	FSRQ	PKS 1454-354
4FGL J1505.0-3433	226.26	−34.55	642.8	3.77e-10	2.15e-08	BLL	PMN J1505-3432
4FGL J2351.4-2818	357.87	−28.31	290.7	1.28e-10	–	–	–
4FGL J0420.3-3745	65.09	−37.75	1841.0	**1.09e-09**	3.43e-08	BCU	NVSS J042025-374443
4FGL J0428.6-3756	67.17	−37.94	24240.3	**2.36e-08**	3.57e-07	BLL	PKS 0426-380
4FGL J1504.4+1029	226.10	10.50	25352.5	**2.02e-08**	9.72e-07	FSRQ	PKS 1502+106
4FGL J0946.2+0104	146.57	1.07	201.8	2.15e-10	–	BLL	1RXS J094620.5+010459
4FGL J0948.9+0022	147.24	0.37	7769.2	**2.29e-09**	1.61e-07	NLSY1	PMN J0948+0022*

Searching for temporary gamma-ray dark blazars associated with IceCube neutrinos

(Kun, Bartos, Becker-Tjus, Biermann, Franckowiak, Halzen, Mező, 2023, A&A, in print)

Matched positions of point sources in the Fermi 4FGL-DR2 catalog with track-type neutrinos from Giommi et al. (2020)

Table 2. Source properties of neutrino source candidates from 4FGL-DR2 being considerable bright in our observational window of one year ($F_{1000} > 10^{-9}$ ph cm^{-2} s^{-1}, see with boldface in Table 1).

Source	4FGL ID	RA (°)	Dec (°)	Class	z	ID$_\nu$	RA$_\nu$ (°)	DEC$_\nu$ (°)	$T_{\mathrm{MJD},\gamma}$ (days)
(1)	(2)	(3)	(4)	(5)	(6)	(7)	(8)	(9)	(10)
RBS 0958	J1117.0+2013	169.27	20.23	BLL	0.1379	IC-130408A	$168.16^{+2.87}_{-1.9}$	$20.67^{+1.15}_{-0.89}$	[56207.6–56572.8]
GB6 J1040+0617	J1040.5+0617	160.15	6.28	BLL	0.7351	IC-141209A	$159.81^{+0.84}_{-1.04}$	$6.57^{+0.64}_{-0.56}$	[56817.5–57182.8]
PKS 1313-333	J1316.1-3338	199.03	−33.64	FSRQ	1.210	IC-160814A	$199.39^{+2.43}_{-3.03}$	$-32.4^{+1.39}_{-1.21}$	[57432.3–57797.5]
TXS 0506+056	J0509.4+0542	77.36	5.70	BLL	0.3365	IC-170922A	$77.43^{+0.95}_{-0.65}$	$5.72^{+0.5}_{-0.3}$	[57836.2–58201.5]
PKS 1454-354	J1457.4-3539	224.37	−35.65	FSRQ	1.424	IC-181014A	$224.3^{+1.4}_{-2.85}$	$-34.8^{+1.15}_{-1.85}$	[58222.9–58588.1]
NVSS J042025-374443	J0420.3-3745	65.09	−37.75	BCU	0.300	IC-190504A	$65.79^{+1.23}_{-1.23}$	$-37.44^{+1.23}_{-1.23}$	[58425.1–58790.4]
PKS 0426-380	J0428.6-3756	67.17	−37.94	FSRQ	1.111	IC-190504A	$65.79^{+1.23}_{-1.23}$	$-37.44^{+1.23}_{-1.23}$	[58425.1–58790.4]
PKS 1502+106	J1504.4+1029	226.10	10.50	FSRQ	1.839	IC-190730A	$225.52^{+1.28}_{-1.43}$	$10.47^{+1.14}_{-0.89}$	[58512.2–58877.5]

Notes. The columns are: (1) source name, (2) 4FGL source ID, (3) right-ascension (J2000, in degrees), (4) declination (J2000, in degrees), (5) type, (6) redshift, (7) neutrino ID (8), neutrino right-ascension (J2000), (9) neutrino declination (J2000), (10) time window for *Fermi*-LAT analysis.

8 of them were bright enough to get a good photon statistics in a one year long time range centered on the respective neutrino detection

Binned likelihood analysis of the Fermi-LAT data of 8 neutrino source candidate blazars (associated with 7 events)

Technical information:

- Dedicated project on a cluster of 16x2.2 GHz Intel Skylake vCPUs (PI: EK), ELKH Cloud (Hungary, Wigner Data Center), using Docker technology (now we have 64 cores)

Software packages: fermipy v1.0.1, ScienceTools v2.0.8 (FermiBottle)

- Instrument response function: P8R3_SOURCE_V2_v1
- Galactic interstellar emission model: gll_iem_v07.fits
- Isotropic diffuse emission model: iso_P8R3_SOURCE_V2_v1.txt

- ROI=15^{o}, evtype=3 (front and back), evclass=128

- Standard quality cuts (zmax=90, (DATA_QUAL > 0) &&(LAT_CONFIG==1))
- Minimum separation between two new point sources: 0.3 deg, TS_{min}=25 (~5sigma)
- Adaptive binning (Lott et al. 2012, 15%)

- Proximity of Sun was checked (with the threshold of 15 degrees)

Flaring behavior is not typical for neutrino source candidate blazars

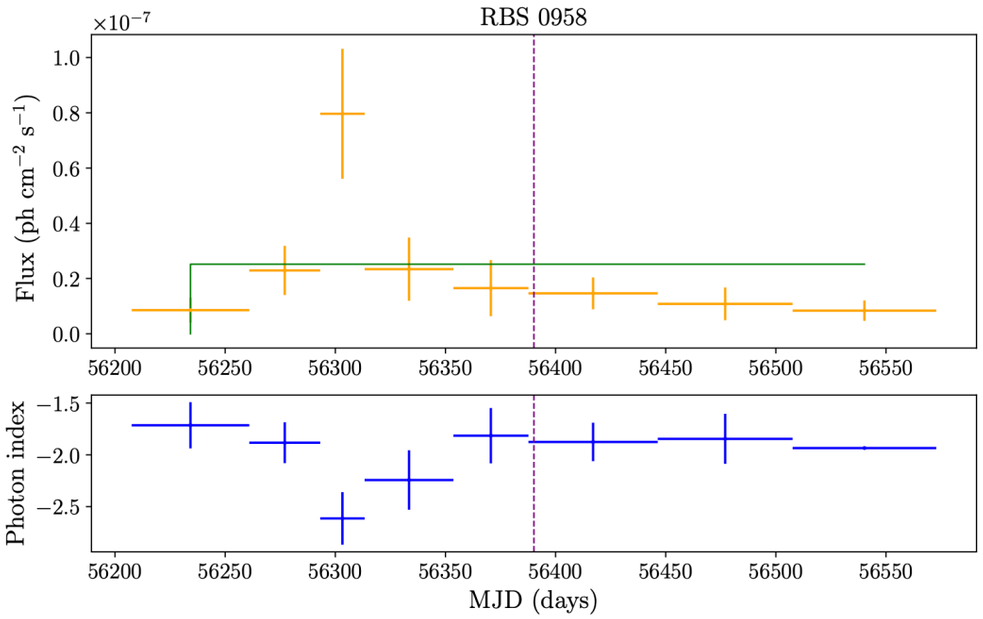

Fig. B.1. Upper panel: Likelihood light curve of RBS 0958 with Bayesian blocks (p = 0.05). The green continuous line represents the Bayesian blocks binning. Lower panel: Photon index as function of time.

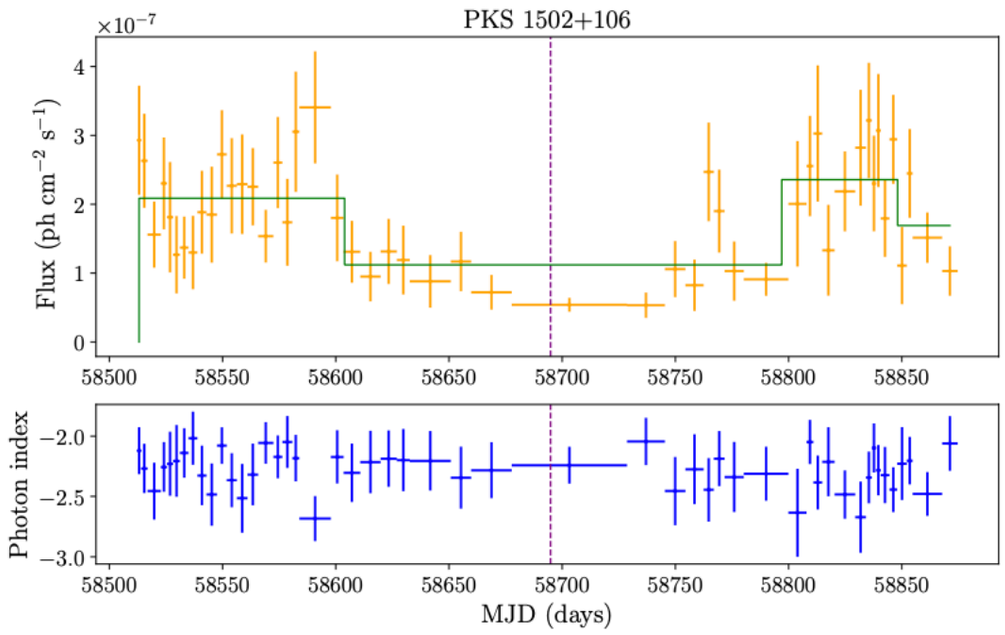

Fig. B.8. Upper panel: Likelihood light curve of PKS 1502+106 with Bayesian blocks (p = 0.05). The green continuous line represents the Bayesian blocks binning. Lower panel: Photon index as function of time.

the only blazar with elevated gamma-ray flux

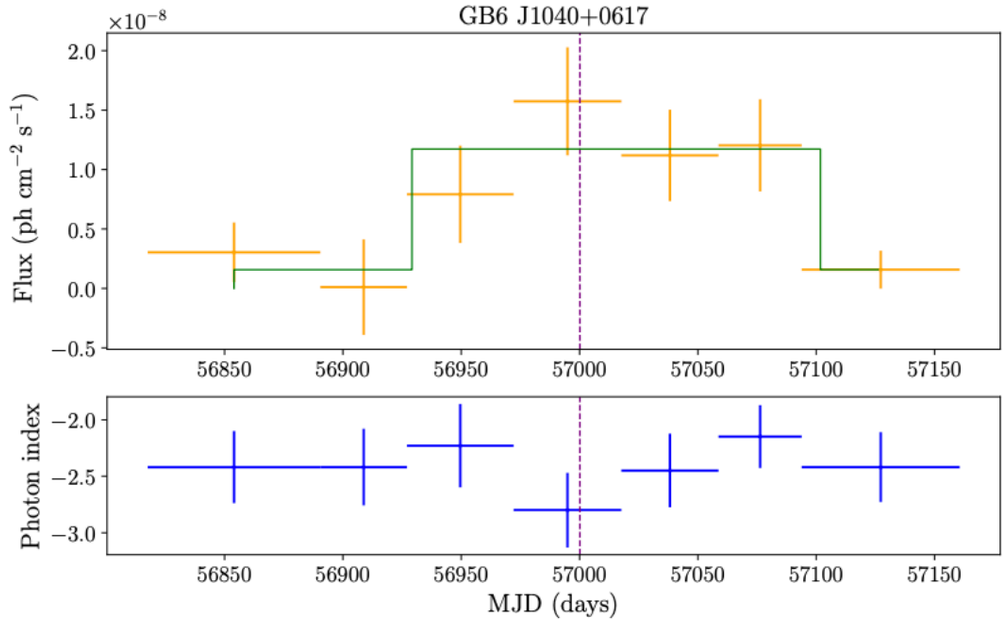

Fig. B.2. Upper panel: Likelihood light curve of GB6 J1040+0617 with Bayesian blocks (p = 0.05). The green continuous line represents the Bayesian blocks binning. Lower panel: Photon index as function of time.

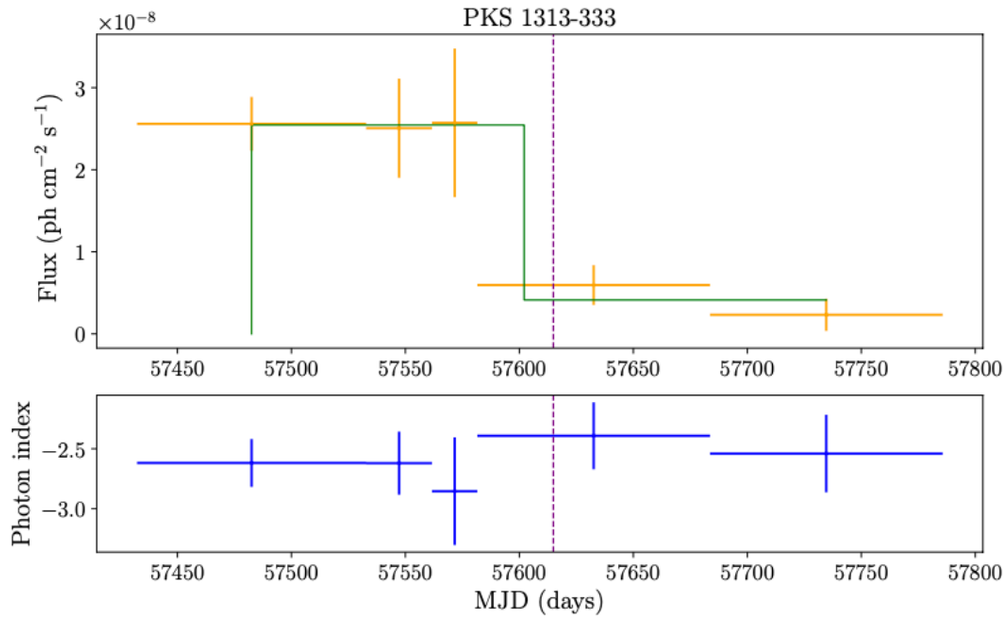

Fig. B.3. Upper panel: Likelihood light curve of PKS 1313-333 with Bayesian blocks (p = 0.05). The green continuous line represents the Bayesian blocks binning. Lower panel: Photon index as function of time.

Flaring behavior is not typical for neutrino source candidate blazars

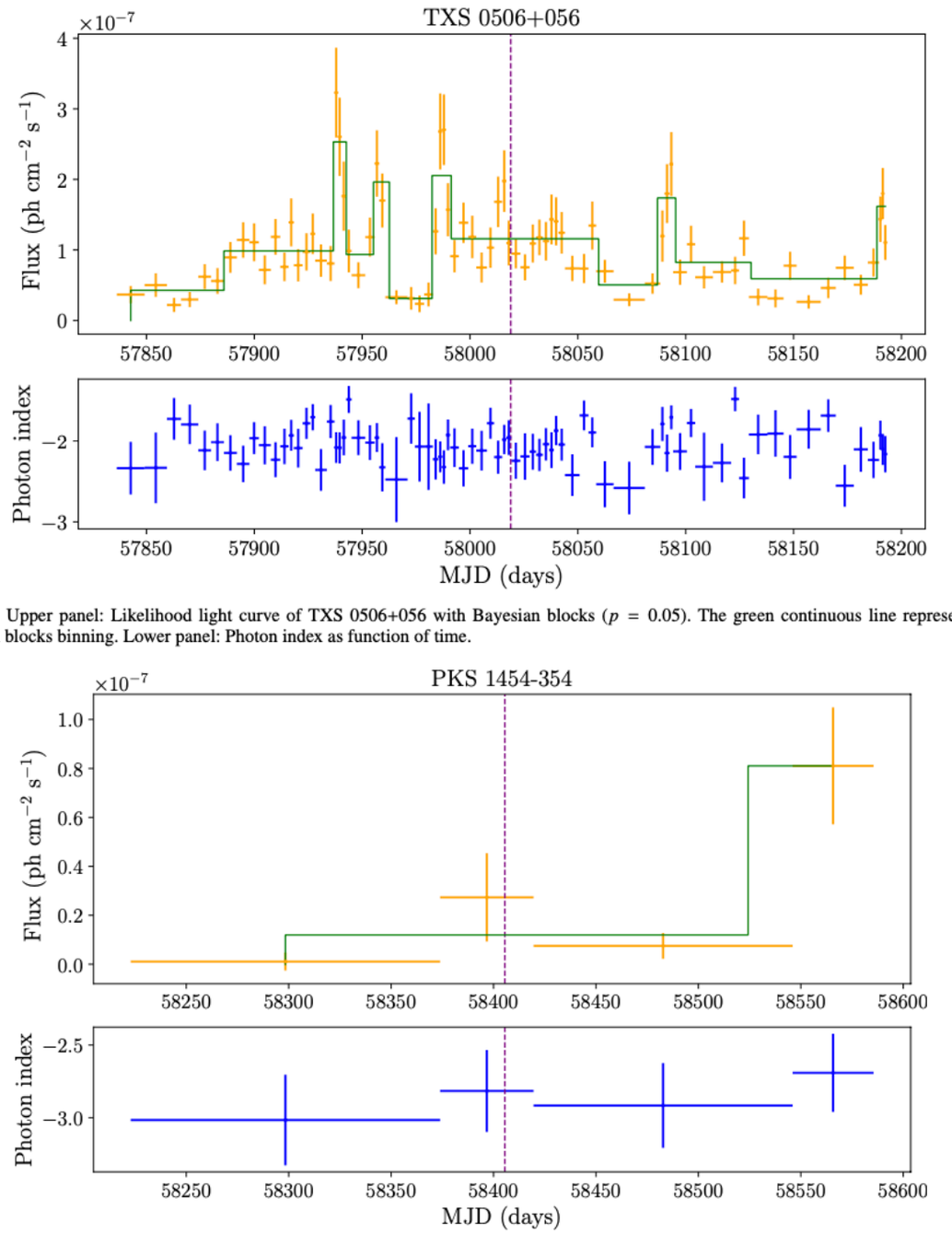

Fig. B.4. Upper panel: Likelihood light curve of TXS 0506+056 with Bayesian blocks ($p = 0.05$). The green continuous line represents the Bayesian blocks binning. Lower panel: Photon index as function of time.

Fig. B.5. Upper panel: Likelihood light curve of PKS 1454-354 with Bayesian blocks ($p = 0.05$). The green continuous line represents the Bayesian blocks binning. Lower panel: Photon index as function of time.

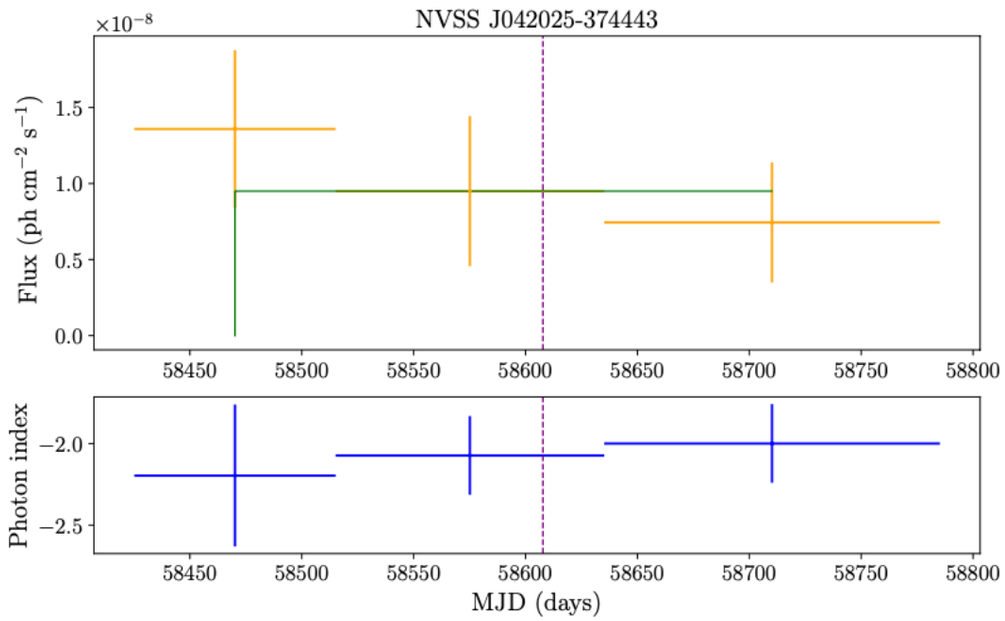

Fig. B.6. Upper panel: Likelihood light curve of NVSS J042025-374443 with Bayesian blocks ($p = 0.05$). The green continuous line represents the Bayesian blocks binning. Lower panel: Photon index as function of time.

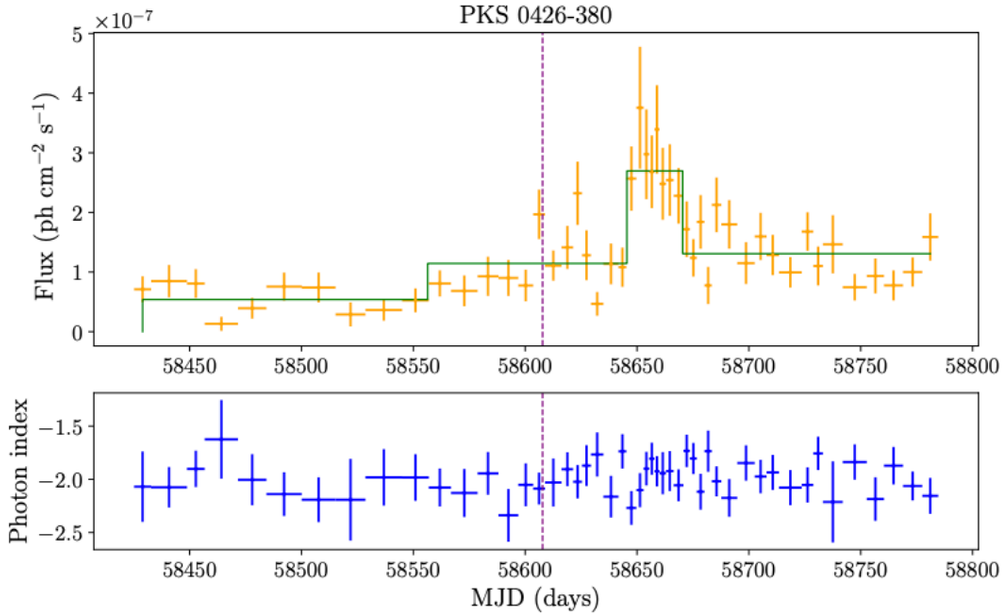

Fig. B.7. Upper panel: Likelihood light curve of PKS 0426-380 with Bayesian blocks ($p = 0.05$). The green continuous line represents the Bayesian blocks binning. Lower panel: Photon index as function of time.

Why we do not see gamma-ray flares during the neutrino detection?

Source	N	$t_{F\nu}$	F_ν	$t_{\mathrm{Fmin}} - t_{F\nu}$	F_{min}/F_ν	$t_{\mathrm{Fmax}} - t_{F\nu}$	F_{max}/F_ν	p
(–)	(–)	(MJD)	(ph cm^{-2} s^{-1})	(days)	(–)	(days)	(–)	(–)
(1)	(2)	(3)	(4)	(5)	(6)	(7)	(8)	(9)
RBS 0958	8	56417.0	$(1.46 \pm 0.58) \times 10^{-8}$	123.2	0.57 ± 0.34	−113.8	5.46 ± 2.70	0.519
GB6 J1040+0617	8	56994.9	$(1.57 \pm 0.46) \times 10^{-8}$	−86.1	0.01 ± 0.26	0.0	1.00 ± 0.41	0.133
PKS 1313-333	5	57632.6	$(5.94 \pm 2.44) \times 10^{-9}$	102.1	0.39 ± 0.37	−61.0	4.36 ± 2.34	0.701
TXS 0506+056	76	58018.0	$(1.10 \pm 0.32) \times 10^{-7}$	−155.2	0.20 ± 0.11	−80.1	2.94 ± 0.99	0.386
PKS 1454-354	4	58396.7	$(2.73 \pm 1.80) \times 10^{-8}$	−98.30	0.04 ± 0.14	169.03	3.00 ± 2.19	0.372
NVSS J042025-374443	3	58575.1	$(9.50 \pm 4.93) \times 10^{-9}$	135.0	0.78 ± 0.58	−105.0	1.43 ± 0.92	0.539
PKS 0426-380	49	58607.8	$(1.97 \pm 0.41) \times 10^{-7}$	−143.6	0.07 ± 0.06	43.5	1.91 ± 0.65	0.219
PKS 1502+106	50	58703.2	$(5.40 \pm 1.01) \times 10^{-8}$	0.00	1.00 ± 0.26	−112.3	6.31 ± 1.91	0.935

$$p = P(F_{\gamma,max} > F_{\gamma,\nu}) = \frac{\Sigma_i \int_{F_{\gamma,\nu}}^{\infty} \mathcal{N}(x, F_i, \sigma_i) dF x}{\Sigma_i \int_{-\infty}^{\infty} \mathcal{N}(x, F_i, \sigma_i) dF x}$$

the probability to randomly pick a bin with higher flux than the neutrino bin

$\mathcal{N}(x, F_i, \sigma_i)$: Gaussian evaluated at x (time), and we assume the uncertainty of the flux is normally distributed

- Sources in our sample are not the sources of the corresponding IceCube neutrinos
- In-source effects (e.g. gamma-ray suppression due to high gamma-gamma opacity)
- Or a combination of these

We plan to conduct a similar study at higher energies with MAGIC and VERITAS data with an updated list of track neutrinos

Do we still need jets?

Recently, Neronov, Savchenko and Semikoz (2023) showed the scaling between the hard X-ray flux (14-195 keV Swift-BAT) and IceCube neutrinos.

NGC 1068 teaches us about the neutrino emission in Seyfert galaxies.
It's faint with Fermi-LAT, and bright with Swift-BAT.

What if Seyferts are steady sources, they show gamma-ray absorption, cascades to hard X-rays, neutrino emission all the time (uniform time PDF), therefore cumulatively they can explain the diffuse neutrino sky detected by IceCube.

What if blazars are more transient sources, they just flash up in neutrinos
(e.g. star wanders through the jet, component ejection, etc..),
and they can explain rather the high-energy triggers of IceCube?

Lots of questions, ton of work to do
We also started to do a neutrino stacking analysis

Thank you for your attention!

Backup slides

Additional point sources found in the ROI of the target sources

Table A.1. Additional sources in the ROI about the target sources. Source ID (1), right-ascension J2000 (2), declination J2000 (3), offset of the new source to the target source (4), flux measured by Fermi between 0.1 GeV and 100 GeV (5), error of the flux value (6), TS-value of the detection (7), predicted number of photons (8).

Source ID	RA	DEC	Δd	$F_{1000} \times 10^{10}$	err$F_{1000} \times 10^{10}$	TS	N_{pred}
-	(°)	(°)	(°)	(ph cm^{-2} s^{-1})	(ph cm^{-2} s^{-1})	-	-
(1)	(2)	(3)	(4)	(5)	(6)	(7)	(8)
RBS 0958							
PS J1106.9+2708	166.719	27.139	7.29	2.39	1.13	18.38	154.21
PS J1132.6+2738	173.161	27.642	8.219	7.80	1.97	58.02	60.53
GB6 J1040+0617							
PS J1042.6+0838	160.655	8.637	2.405	7.89	1.72	441.27	615.38
PKS 1313-333							
PS J1242.8-2554	190.720	-25.912	10.557	5.07	1.70	8.1	32.42
PS J1246.4-2602	191.610	-26.039	9.950	8.68	0.12	60.65	123.66
TXS 0506+056							
PS J0500.7-0140	75.183	-1.671	7.686	22.32	0.18	365.95	383.90
NVSS J042025-374443							
PS J0347.8-3618	56.952	-36.316	6.654	4.62	1.25	40.84	147.55
PS J0348.7-3029	57.184	-30.484	9.774	3.06	1.01	131.58	424.67
PS J0454.4-3140	73.614	-31.667	9.271	2.44	1.09	20.71	133.68
PKS 0426-380							
PS J0456.4-4318	74.113	-43.302	7.511	3.80	1.31	53.98	370.24
PKS 1502+106							
PS J1446.6+1213	221.652	12.216	4.690	3.37	0.14	16.96	60.75
PS J1525.8+1636	231.470	16.605	8.030	4.14	0.33	48.66	350.34

The proposed scenario

$p\gamma$ in jets, pp is probably subdominant because of the lower particle densities

The flavor-averaged diffuse high-energy cosmic neutrino flux is related to cosmic-ray flux:

$$\frac{1}{3}\sum_{\alpha} E_\nu^2 \frac{dN_\nu}{dE_\nu} \simeq \frac{c}{4\pi}\left(\frac{1}{2}(1 - e^{-\tau_{p\gamma}})\xi_z t_H \frac{dE}{dt}\right)$$

The IceCube all-flavor diffuse neutrino flux: ~3×10^{-11} TeV cm^{-2} s^{-1} sr^{-1}

The injection rate of cosmic rays above 10^{16} eV: $dE/dt\sim1\text{-}2\times10^{44}$ erg Mpc^{-3} yr^{-1}

Lead to optical depth for $p\gamma$ interactions as: $\tau_{p\gamma}$ ~0.4
(assuming that muon neutrino emission rate follows a power law $E^{-\Gamma}$, where Γ=2.19

$$\tau_{\gamma\gamma} \approx \frac{\eta_{\gamma\gamma}\sigma_{\gamma\gamma}}{\eta_{p\gamma}\hat{\sigma}_{p\gamma}}\tau_{p\gamma} \quad \Longrightarrow \quad \tau_{\gamma\gamma} \sim \mathcal{O}(100)$$

Theory suggests a gamma-ray flare is not expected when the source is a highly efficient neutrino emitter, since the gamma-gamma opacity is about 2 orders of magnitude larger than the gamma-proton opacity, that can explain the CR and neutrino observations.

The proposed scenario

$p\gamma$ in jets, pp is probably subdominant because of the lower particle densities

- Astrophysical muon neutrino energies (E_μ) 119 TeV- 4.8 PeV correspond to proton energies (E_p) 2.4 PeV — 96 PeV ($E_p \approx 20 E_\mu$)

- Assuming the meson production is dominated by Delta-resonance, these protons interact with X-ray and UV target photons, constraining the two-photon annihilation depth at $E_\gamma \sim 5 - 200\ \mathrm{GeV}$ (compatible with Fermi-LAT)

- 5-200 GeV photons produce e^+e^- pairs with $10\ \mathrm{keV}(\gamma/10)^2 - 3\mathrm{eV}(\gamma/10)^2$ photons

- In blazar jets the electron Lorentz factor is highly relativistic, rendering the energy of photons absorbing the pionic gamma-rays to keV, MeV or even GeV regime

- We expect *temporary neutrino emission, gamma-ray absorption, X-ray flare*